soil systems

MDPI

Article

Tracing Soil Contamination from Pre-Roman Slags at the Monte Romero Archaeological Site, Southwest Spain

Juan Carlos Fernández-Caliani [1,*] and Juan Aurelio Pérez-Macías [2]

[1] Department of Earth Sciences, University of Huelva, Campus de El Carmen, 21071 Huelva, Spain
[2] Department of History, Geography, and Anthropology, University of Huelva, Campus de El Carmen, 21071 Huelva, Spain; japerez@uhu.es
* Correspondence: caliani@uhu.es

Abstract: Soil serves as a repository of human history, preserving artifacts within its horizons. However, the presence of chemically reactive remnants, such as ancient slags, can significantly impact the surrounding soil environment. This paper addresses this scarcely explored issue by focusing on soil contamination arising from pre-Roman slag deposits at the Monte Romero archaeological site in southwest Spain, dating back to the Tartessian period (c. 7th century BC). Through the high-resolution microscopy examination of slag wastes and the trace element analysis of soil samples by ICP-OES, this study evaluated current contamination status using a multi-index approach. The results revealed markedly high levels of Pb (>5000 mg kg^{-1}), Cu (up to 2730 mg kg^{-1}), and As (up to 445 mg kg^{-1}) in the soil compared to a control sample. The identification of secondary complex compounds like Cu arsenates and Pb arsenates/antimonates within slag cavities suggests post-depositional weathering processes, leading to the dispersion of potentially toxic elements into the surrounding soil. Assessments through indices of contamination and potential ecological risk highlighted severe contamination, particularly concerning Ag, Pb, Sb, Cu, and As. This study underscores the importance of addressing potential environmental hazards associated with archaeological sites hosting remnants of metal production.

Keywords: trace elements; archaeometallurgy; pre-Roman slags; Tartessos; Iberian Pyrite Belt

Citation: Fernández-Caliani, J.C.; Pérez-Macías, J.A. Tracing Soil Contamination from Pre-Roman Slags at the Monte Romero Archaeological Site, Southwest Spain. *Soil Syst.* **2024**, *8*, 78. https://doi.org/10.3390/soilsystems8030078

Academic Editor: Antonio Martínez Cortizas

Received: 20 May 2024
Revised: 1 July 2024
Accepted: 5 July 2024
Published: 8 July 2024

1. Introduction

Soil plays a critical role in biogeochemical cycling, sustaining life and providing ecosystem services. It also serves as a repository of our archaeological and geological heritage, hosting anthropogenic artifacts of cultural value that offer insights into ancient human activities [1]. However, these artifacts can become sources of environmental contamination, depending on their composition and reactivity within the soil matrix. Archeometallurgical materials often contain elevated concentrations of potentially harmful elements [2,3], posing significant threats to soil quality. Abandoned settlements with long histories of mining and metallurgical activities provide valuable opportunities to study the long-term fate and behavior of pollutants within the soil system [4]. Therefore, assessing the concentration of trace elements in soils near archaeological settings displaying indications of potential contamination is a pertinent matter of study.

Soil and sediment contamination by heavy metals derived from metallurgical waste dumps have been documented in the literature for a number of historical smelting sites across various regions, including Britain [5], Central Europe [3,6], Australia [7], South America [8], and prominent ore districts, such as the *Colline Metallifere* district in southern Tuscany [9] and the Iberian Pyrite Belt [10–12].

In metalliferous regions like the Iberian Pyrite Belt, situated in the southwest of the Iberian Peninsula, mining and extracting copper and silver significantly contributed to the civilization and development of ancient societies [13,14], but has also left adverse environmental legacies. Over centuries of intensive smelting activities during the Roman

era, vast quantities of metallurgical waste, estimated at around 30 million tons [15], were generated. These wastes were disposed of near mining sites, forming extensive slag heaps. Evidence of pre-Roman smelting activities is also apparent, with an estimated 4 million tons of slag inferred from surface deposits [16]. Remnants of ancient metallurgical processes are scattered across southwest Iberia, with notable concentrations found in Rio Tinto, where 6 million tons of copper and silver slags are piled up in the soil [17]. Over time, fractions of arsenic and heavy metals, typically present in metallurgical wastes [18,19], might have migrated into the surrounding ecosystems, potentially causing significant contamination.

While the environmental impact of modern mining practices in the Iberian Pyrite Belt is well documented [20–22], and references therein, research concerning soil contamination arising from ancient smelting activities remains notably scarce. This study aimed to address this knowledge gap by examining the current level of soil contamination around the Monte Romero protohistoric smelter and assessing the potential ecological risks associated with the identified trace elements of concern.

2. The Archeological Site of Monte Romero

Monte Romero (37°46′37″ N–6°47′33″ W) is situated in the province of Huelva (Spain), within the municipality of Almonaster la Real, approximately 1 km southwest of the Cueva de la Mora mining village (Figure 1).

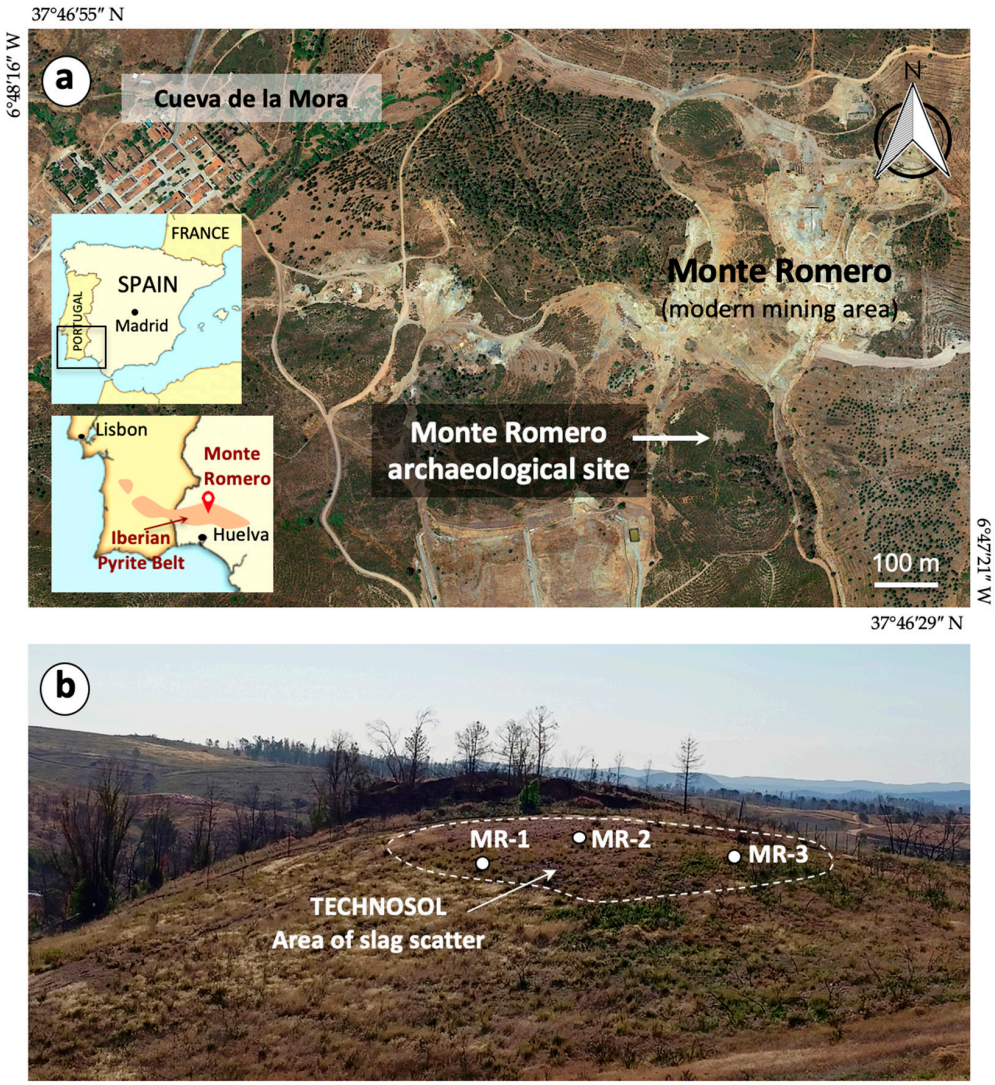

Figure 1. Geographic setting of Monte Romero, showing (**a**) the archaeological site and (**b**) the sampling locations within the site.

Geologically, it lies in the northernmost part of the Iberian Pyrite Belt, renowned as one of the world's largest volcanogenic massive sulfide provinces. The Monte Romero orebody is a polymetallic (Pb-Zn-Cu-Ag) massive sulfide deposit hosted in a volcanic–sedimentary sequence dominated by felsic volcanic rocks [23]. The deposit was primarily mined for copper, yielding 600,000 tons of ore during the first third of the 20th century [24]. Past mining and ore processing activities have resulted in significant deforestation, leading to the destruction of natural vegetation and the conversion of soils into marginal lands, currently supporting sparse vegetation or remaining barren. Eutric Cambisol is the dominant soil group developed on the felsic volcanic rocks [25], although large parts of natural soils have been transformed into mine Technosols. The region has a Mediterranean continental climate with some Atlantic influences, and is characterized by hot, dry summers, and mild, wet winters.

The protohistoric smelter was first discovered in 1975 near the modern mining area of Monte Romero, during the Huelva Archaeo-Metallurgical Exploration Project [26]. The archaeological survey at Monte Romero unveiled extensive traces of silver and copper smelting activities. Two distinct types of slag were recovered: (1) free-silica (quart-bearing), plano-convex slags, characterized by a spherical shape with a flattened underside; and (2) flat slags displaying a casting structure and significant matte content. Based on field observations, the volume of the slag deposit is estimated to be roughly 300 m^3, with an average density of 3.6 g cm^{-3}, resulting in a total mass of about 1080 tons. Other archaeological finds included grooved stone mining tools, tuyeres bearing litharge impregnations, and fragments of copper–silver matte ([13], p. 123). The archaeological excavation conducted in 1986 [27] led to the conclusion that Monte Romero served as an important mining center and metallurgical workshop linked to the production of silver and copper from complex polymetallic sulfide ores [28].

The Monte Romero archeological site has been listed in the General Catalog of Andalusian Historical Heritage since 2005 [29]. At this site, all stages of mineral processing, from polymetallic ore extraction to cupellation, were conducted through a sophisticated pyrometallurgical process ([13], p. 127) [30,31]. Typological analyses of broken pieces of ceramic materials found at the site, including handmade decorated vessels and Phoenician amphorae, date this protohistoric settlement to the mid-7th to early 6th centuries BC [32]. This period, locally termed the Tartessian period, corresponds to the Orientalizing Late Bronze Age, and marked the establishment of trading links between southwestern Iberia and the Eastern Mediterranean.

3. Materials and Methods

3.1. Sampling and Sample Preparation

Three composite soil samples (MR-1, MR-2, and MR-3) were collected from a barren area (20 × 30 m) within the archaeological site boundaries (Figure 1). This area corresponds to the location of a former smelting workshop, as indicated by the occurrence of scattered slags within the collected soil. Concurrently, representative samples of the slags were also gathered from the same sampling points. In addition, a control soil sample (BJ-0) was obtained from a location (37°47′07″ N–6°48′51″ W) positioned outside the modern mining area of Monte Romero, roughly 2 km northwest of the archaeological site. This control sample showed no discernible signs of contamination and served as a benchmark for comparison.

At each sampling site, three discrete samples were collected from the topsoil layer (0–10 cm depth) using a polypropylene hand shovel. The samples were combined in the field to create composite samples weighing approximately 3 kg, and were stored in zip-lock polyethylene bags. Upon reaching the laboratory, the composite samples were spread out on absorbent paper and left to air-dry at room temperature. After drying, mechanical disaggregation was performed with a wooden roller, followed by homogenization and sieving through a 2 mm mesh sieve to obtain a consistent particle size fraction. Representative subsamples were formed by coning and quartering. An aliquot was then finely ground

in an agate mortar and passed through a 63 µm sieve to achieve a uniform powder for chemical analysis.

3.2. Soil Texture and Electrochemical Properties

Soil texture was determined using particle-size distribution data obtained from laser diffraction analysis performed on a Mastersizer 3000 analyzer (Malvern Instruments Ltd., Worcestershire, UK). Potentiometric measurements of pH and electrical conductivity were conducted by stirring 10 g of soil in 25 mL of deionized water for 5 min, followed by a standing period of 30 min. pH measurements were carried out using a Crison Basic 20 pH meter with a glass electrode calibrated with pH 4 and 7 buffer solutions at 25 °C. Electrical conductivity measurements were conducted using a Crison GLP 31 conductivity meter equipped with a glass electrode calibrated with two standard KCl solutions.

3.3. Bulk Chemical Analysis

The soil samples underwent a multi-acid digestion process ($HClO_4$ + HNO_3 + HF + HCl) and the resulting extract solutions were analyzed by inductively coupled plasma optical emission spectrometry (ICP-OES) at Activation Laboratories (Ancaster, ON, Canada). This laboratory adheres to ISO/IEC 17,025:2017 standard [33], ensuring the reliability and quality of the analytical results. In this study, we analyzed the total concentrations of 19 trace elements, including Ag and several environmentally significant elements, such as As, Bi, Cd, Co, Cr, Cu, Ni, Pb, Sb, and Zn.

The quality of the analytical procedure was controlled by certified reference materials from the OREAS series (13b, 45d, 70b, 72b, 77b, 96, 98, 101b, 247, 521, 620, 681, 753, and 904), reagent blanks, and replicate samples to verify the accuracy and reproducibility of the data (Table S1). The relative standard deviations from duplicates and the certified values for the majority of the reported elements were found to be less than 10%, indicating high data quality.

3.4. High-Resolution Microscopy and Microchemical Analysis

To analyze the composition and microstructure of the slag samples, they were carefully fragmented to expose fresh surfaces. Selected fragments were then coated with a thin layer of carbon to enhance their electrical conductivity and examined using a field-emission scanning electron microscope (FESEM) equipped with an energy-dispersive X-ray spectroscopy (EDS) microanalysis system and detectors for secondary and backscattered electrons. The FESEM (JSM-IT500HR instrument, JEOL, Tokyo, Japan) operated under standard conditions with an accelerating voltage of 20 kV, a working distance of 10 mm, and a variable beam diameter tailored to the size of the analyzed particle.

3.5. Indices of Contamination and Potential Ecological Risk

Soil contamination by trace elements was assessed using various indices, including the degree of contamination proposed by Hakanson [34], the pollution load index introduced by Tomlinson et al. [35], and the ecological risk index, also suggested by Hakanson [34]. Based on the contamination degree index, Abrahim and Parker [36] classified the contamination level into seven grades, ranging from nil to very low contamination ($Cd < 1.5$) to ultra-high degree of contamination ($Cd \geq 32$).

These indexes rely on the contamination factor (Cf), computed by dividing the concentration of each element in the soil (C_s) by its concentration in the control sample, taken as the local background value (C_b), as shown in Equation (1):

$$Cf = \frac{C_s}{C_b} \quad (1)$$

In this study, the control sample BJ-0 was used as a reference.

The degree of contamination (*Cd*) was obtained by summing the individual contamination factors (*Cfi*), as follows (Equation (2)):

$$Cd = \sum_{i}^{n} Cfi \quad (2)$$

The pollution load index (PLI) was derived from the geometric mean of the contamination factors (*Cf*) for the elements of concern, as described in Equation (3):

$$\mathrm{PLI} = \left(C_{f\,Ag} \times C_{f\,As} \times C_{f\,Bi} \times C_{f\,Cd} \times C_{f\,Cu} \times C_{f\,Pb} \times C_{f\,Sb} \right)^{\frac{1}{7}} \quad (3)$$

The potential ecological risk index (ERI), primarily driven by contaminants such as *As*, *Cd*, *Pb*, and *Cu* [34], was computed using Equation (4):

$$\mathrm{ERI} = \sum_{i}^{n} Cfi \times Tfi \quad (4)$$

where ERI is the potential ecological risk, *Cfi* denotes the contamination factor of element *i*, and *Tfi* indicates the corresponding toxicological factor according to Häkanson [34] (*As* = 10, *Cd* = 30, *Cu* = *Pb* = 5). Based on the ERI values, the following grades were used to describe the potential ecological risk: low risk (ERI < 150); moderate risk (150 ≤ ERI < 300); considerable risk (300 ≤ ERI < 600); and very high risk (ERI ≥ 600).

4. Results and Discussion

4.1. Slag Description

The macroscopic examination of the slag samples revealed distinctive globular and oval morphologies (Figure 2). Upon fracturing, the freshly exposed surfaces displayed a dark gray or black glassy matrix containing numerous, visible (naked eye) irregularly shaped grains of quartz. These features, including the presence of ball-shaped slags with flattened bases, are strongly indicative of free-silica (unreacted quartz) silver slag, a type commonly produced in the Iberian Peninsula during the Tartessian period [37,38]. Similar slags have been documented in the archaeological site of Monte Romero [26,27] and other settlements and production centers across southwest Iberia ([5], pp. 79–154) [38].

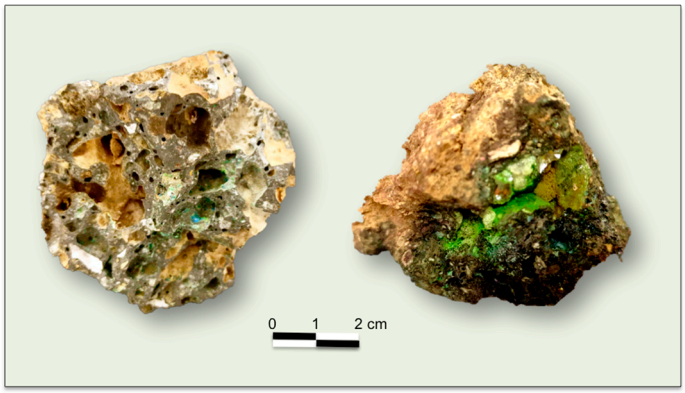

Figure 2. General appearance of the free-silica silver slags recovered from Monte Romero.

Chemical analyses of three free-silica type slags from Monte Romero (samples PH–146, PH–148, and PH–160), as reported by Rothenberg and Blanco [26], yielded an average composition of 22.4% silica (SiO_2); 19.93% Fe; 3.80% Pb; 0.97% S; 0.67% Cu; 0.50% Zn; 0.17% As; 0.16% Sb; and 87 mg kg^{-1} Ag.

Based on the above metal contents, the slag heaps at Monte Romero contain approximately 41 t of Pb, 7.2 t of Cu, 5.4 t of Zn, 1.8 t of As, and 90 kg of Ag. To contextualize these figures, the total mass of slag (~1080 t) and contained metals at this archaeological site is significantly smaller than modern slag dumps in the Iberian Pyrite Belt. Contemporary copper smelting operations typically produce slag materials that are several orders of

magnitude greater. For instance, the slag dumps adjacent to the derelict pyritic smelter complex of Rio Tinto (10 million tons) contain 43 t of Ag, 1100 t of As, 44,100 t of Cu, and 20,900 of Pb [10]. Similarly, the slags generated at São Domingos (4.7 million tons) contain approximately 1000 t of As, 16,000 t of Cu, 14,000 t of Pb, and 40,000 t of Zn [39]. The Monte Romero site represents historical pollution from smaller-scale operations with lower technological capabilities, leading to less efficient metal extraction and higher residual metal content in the slag, particularly Ag, Cu, and Pb.

Another common feature observed in the slags is the occurrence of numerous vesicles. These are small, spherical or ellipsoidal cavities formed by the entrapment of gas bubbles during slag solidification, similar to those found in volcanic glass. This vesicularity effectively increases the overall surface area of the slag, thereby enhancing its chemical reactivity. Under binocular microscopy, some of these cavities and fissures appear filled or coated with crystalline aggregates of secondary minerals showing greenish and bluish hues (Figure 3). This suggests the precipitation of newly formed minerals within the open spaces.

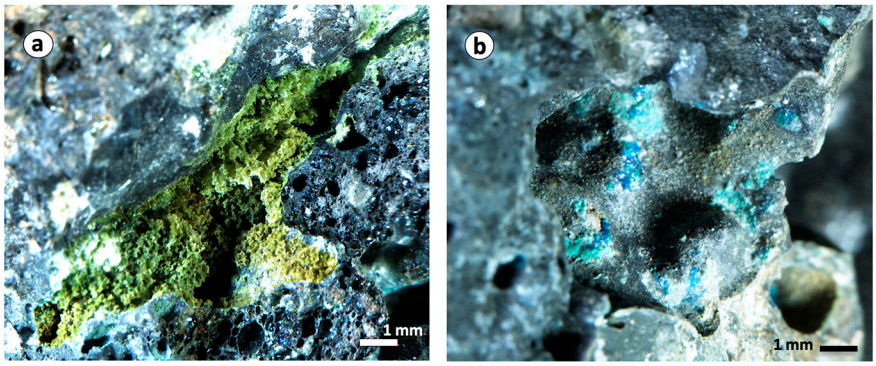

Figure 3. Close-up view of cavities and fissures within the slag, lined with secondary minerals exhibiting (**a**) greenish and (**b**) bluish hues.

Backscattered electron (BSE) images acquired with the FESEM (Figure 4) provided a more detail view of the vesicular surface of the slags and their porous structure, as well as the appearance of minerals precipitated within some vesicles. These minerals exhibited diverse crystalline habits, such as botryoidal (grape-like clusters) and coralloid forms, often forming radial groups of acicular (needle-like) crystals.

Microchemical analysis via the EDS of representative crystals (Table 1) revealed that copper arsenates were the predominant secondary minerals (analyses 3, 4, 5, and 6). These minerals exhibited varying proportions of As and Cu, ranging from 21% to 28% for As and 27% to 56% for Cu. In addition, copper–iron arsenates were identified, containing up to 20% Fe (analysis 1). Lead arsenates/antimonates were also detected (analysis 2 and 7), characterized by a more complex composition, including 8–19% As, 23–25% Pb, and 10–20% Sb, along with lower amounts of copper (4–8% Cu) and iron (<3% Fe), among other elements.

The chemical compositions determined by EDS suggest that these secondary minerals are likely supergene copper arsenates, such as olivenite (Cu_2AsO_4OH), lammerite ($Cu_3[AsO_4]_2$), and rollandite ($Cu_3[AsO_4]_2 \cdot 4H_2O$), commonly found in the oxidized zone of hydrothermal arsenic-bearing copper deposits. However, precise identification through stoichiometric calculations requires quantitative chemical analysis using electron probe microanalysis (EPMA) on polished sections.

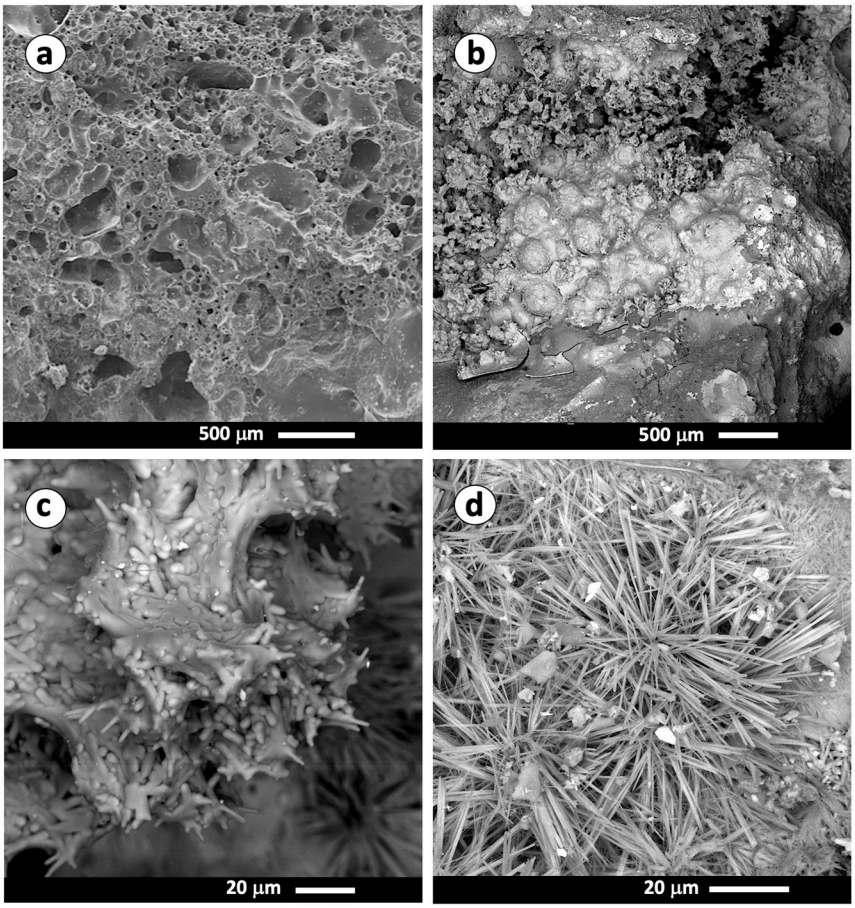

Figure 4. High-resolution FESEM-BSE images depicting (**a**) the vesicular surface of the slag; (**b**) botryoidal habit of secondary minerals; (**c**) coralloid habit of secondary minerals; and (**d**) radial aggregates of acicular olivenite crystals filling a vesicle.

Table 1. Chemical composition (wt%) of representative secondary minerals identified within slag cavities, as determined by energy-dispersive X-ray spectroscopy (EDS).

Element	Analysis Number						
wt%	1	2	3	4	5	6	7
O	32.5 ± 0.5	26.5 ± 0.4	34.6 ± 0.5	35.3 ± 0.6	20.4 ± 0.6	29.4 ± 0.5	35.6 ± 0.6
As	24.0 ± 0.5	8.0 ± 0.2	27.4 ± 0.6	26.1 ± 0.6	21.2 ± 0.7	26.9 ± 0.6	18.5 ± 0.4
Cu	18.6 ± 0.4	8.2 ± 0.2	36.9 ± 0.6	27.2 ± 0.5	56.1 ± 0.8	42.5 ± 0.6	4.5 ± 0.3
Fe	20.1 ± 0.3	2.9 ± 0.1	1.1 ± 0.2	5.1 ± 0.2	2.3 ± 0.2	1.1 ± 0.2	1.3 ± 0.2
Pb	2.4 ± 0.4	23.8 ± 0.4	-	4.1 ± 0.5	-	-	25.1 ± 0.6
Sb	0.6 ± 0.2	20.4 ± 0.3	-	0.9 ± 0.2	-	-	9.5 ± 0.3
Bi	-	5.5 ± 0.5	-	-	-	-	-
Sn	-	2.9 ± 0.1	-	-	-	-	-
Al	-	-	-	-	-	-	4.8 ± 0.2

These secondary minerals may also result from alteration of metallurgical phases within complex slags exposed to weathering for centuries [40]. Slag is inherently porous and chemically reactive, which leads to the formation of secondary minerals through reactions with atmospheric oxygen and surface water, typically under conditions with a pH above 4 [41]. The precipitation of these secondary phases provides evidence of slag weathering and the subsequent release of trace elements into the surrounding soils, as reported in other ancient smelting wastes [3]. At the Monte Romero site, the arsenates filling the slag vesicles can be interpreted as precipitates from meteoric solutions enriched in As and heavy metals. This enrichment likely occurred due the breakdown or destabilization of the primary metallurgical phases of the slags within the soil environment. Dissolution and

recrystallization reactions significantly influence the mobility of metal(loid)s in dumps [7]. The presence of relatively soluble complex arsenates suggests that historical slag wastes pose a potential environmental threat, acting as sources of As and heavy metals that could be released over time. However, it is noteworthy that repeated cycles of dissolution and reprecipitation commonly lead to the formation of the least soluble phases, thereby potentially reducing long-term environmental risks.

4.2. Soil Properties and Total Trace Element Concentrations

Soil samples collected from the archaeological site exhibited a textural class (silt loam) and physicochemical characteristics (slightly acidic reaction and low electrical conductivity) consistent with the control soil. On the other hand, they revealed remarkably higher total concentrations of trace elements, as detailed in Table 2.

Table 2. Soil properties and total concentrations of trace elements analyzed by ICP-OES in the <2 mm fraction of potentially contaminated soil samples and the control sample.

Sample	MR-1	MR-2	MR-3	Mean	BJ-0 (Control)
Soil texture	Silt loam	Silt loam	Silt loam	Silt loam	Silt loam
pH (in water)	6.61	6.09	6.17	6.29 ± 0.28	6.72
EC (μS cm^{-1})	276	286	255	272 ± 16	194
		Element (mg kg^{-1})			
Ag	32.6	40.9	29.4	34 ± 5.9	0.4
As	285	445	378	369 ± 80	68
Be	3	3	3	3.0 ± 0.0	2
Bi	3	4	7	4.7 ± 2.1	1
Cd	1.6	2.5	2.1	2.1 ± 0.5	1.0
Co	10	11	14	12 ± 2.1	22
Cr	41	42	65	49 ± 14	33
Cu	2500	2210	2730	2480 ± 261	383
Ga	22	20	24	22 ± 2.0	18
Li	63	65	69	65.7 ± 3.1	30
Mo	1	2	2	1.7 ± 0.6	1
Ni	23	20	30	24 ± 5.1	23
Pb *	>5000	>5000	>5000	>5000	266
Sb	64	72	81	72 ± 8.5	2.5
Sc	19	18	24	20 ± 3.2	33
Sr	68	79	73	73 ± 5.5	129
Te	2	5	5	3.7 ± 2.3	3
V	48	74	80	67 ± 17	49
W	7	9	8	8.0 ± 1.0	6
Y	58	52	63	58 ± 5.5	40
Zn	505	705	640	617 ± 102	517

* Right-censored Pb values were replaced with the upper limit of quantification (5000 mg kg^{-1}).

In fact, all soil samples hosting the Monte Romero slags exhibited exceptionally high levels of Pb, exceeding the upper limit of quantification (5000 mg kg^{-1}); hence, the Pb contents reported in Table 2 represent minimum estimates. Copper concentrations were also markedly elevated compared to the control sample, with an average value of 2480 mg kg^{-1}. Other trace elements of potential concern, such as Zn reaching up to 705 mg kg^{-1}, and As up to 445 mg kg^{-1}, were also found at relatively high levels. These findings indicate significant contamination with these potentially toxic elements, with total concentrations comparable to those reported in soils around abandoned mine sites in the Iberian Pyrite Belt [22].

The concentrations of the remaining analyzed elements were all below 100 mg kg^{-1}. However, the content of Ag in the soil samples (29.4–40.9 mg kg^{-1}) was notably elevated compared to both the control sample and the average concentration of Ag (0.13 mg kg^{-1}) reported in soils worldwide [42]. This enrichment suggests a potential anthropogenic influence from past metallurgical activities, likely linked to inefficient metal recovery processes.

4.3. Trace Elements of Concern and Potential Ecological Risk

The primary contaminant elements introduced into the soil by the slag wastes (Ag, As, Bi, Cu, Pb, and Sb) are clearly distinguishable when comparing their mean concentrations in the contaminated soil with those in the control soil (Figure 5). This distinct geochemical association is consistent with the chemical composition of the polymetallic ores historically mined at the now-abandoned Monte Romero mine [24].

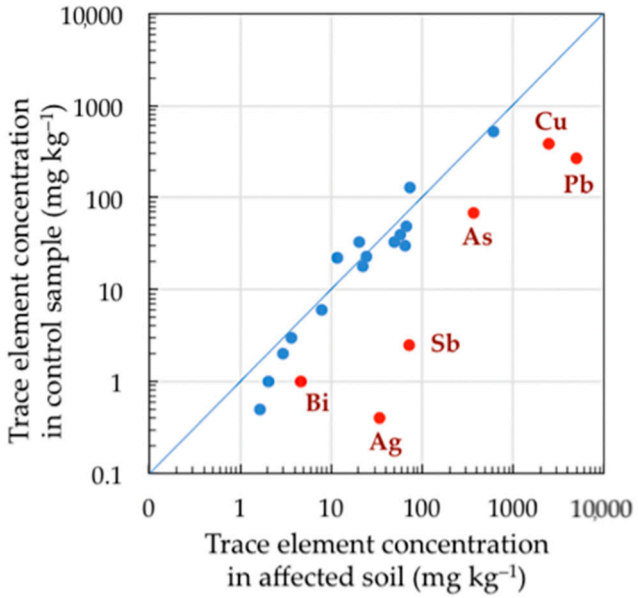

Figure 5. Isocon diagram illustrating the enrichment of trace elements, notably Ag, As, Bi, Cu, Pb, and Sb, in soil hosting the slags. Contaminant elements (red dots) falling below the diagonal line (isoline) indicate their significant enrichment compared to background levels (control sample). The reported Pb content in the affected soil is considered a minimum estimate.

Table 3 summarizes the calculated values of contamination factor (*Cf*), contamination degree (*Cd*), pollution load index (PLI), and potential ecological risk index (ERI).

The results revealed that Ag is the most enriched metal in the soil, with an average *Cf* of 85.75, followed by Sb with an average of 28.93, and Pb with a *Cf* exceeding 18.80 in all samples. The values are indicative of very high contamination. Other trace elements, including Cu, As, and Bi, also showed considerable contamination ($Cf > 4$), though to a lesser extent than in most mine soils of the Iberian Pyrite Belt [22]. The remaining analyzed trace elements generally displayed *Cf* values around unity, suggesting a minimal contribution to overall contamination.

The degree of contamination (*Cd*), derived from the sum of individual *Cf* values for the elements of concern (Ag, As, Bi, Cd, Cu, Pb, and Sb), exceeded 141 in all samples, indicating severe anthropogenic contamination at the site. Similarly, the PLI, calculated from the geometric mean of individual *Cf* values, presented relatively high values ($PLI > 9$), further supporting the conclusion of significant anthropogenic influence.

The right-censored ERI value of 242 surpassed the low ecological risk threshold, indicating moderate-to-high ecological risk [33], although the near-neutral pH level observed in the soil suggests a relatively low potential for metal mobility. This finding is important as it suggests that the contaminants are less likely to migrate through the soil.

Table 3. Contamination factor (*Cf*) for each trace element per sample and their respective averages, alongside multi-elemental contamination indices: degree of contamination (*Cd*), pollution load index (PLI), and ecological risk index (ERI).

Element	MR-1	MR-2	MR-3	Mean
Contamination factor (*Cf*)				
Ag	81.5	102	73.5	85.8 ± 14.8
As	4.19	6.54	5.56	5.43 ± 1.2
Be	1.50	1.50	1.50	1.50 ± 0.0
Bi	3.00	4.00	7.00	4.67 ± 2.1
Cd	1.60	2.50	2.10	2.07 ± 0.5
Co	0.45	0.50	0.64	0.53 ± 0.1
Cr	1.24	1.27	1.97	1.49 ± 0.4
Cu	6.53	5.77	7.13	6.48 ± 0.7
Ga	1.22	1.11	1.33	1.22 ± 0.1
Li	2.10	2.16	2.30	2.19 ± 0.1
Mo	1	2	2	1.6 ± 0.6
Ni	1.00	0.87	1.30	1.06 ± 0.2
Pb	>18.8	>18.8	>18.8	>18.8
Sb	25.6	28.8	32.4	28.9 ± 3.4
Sc	0.58	0.55	0.73	0.62 ± 0.1
Sr	0.53	0.61	0.57	0.57 ± 0.0
Te	0.67	1.67	1.67	1.33 ± 0.6
V	0.98	1.51	1.63	1.37 ± 0.3
W	1.17	1.50	1.33	1.33 ± 0.2
Y	1.45	1.30	1.58	1.44 ± 0.1
Zn	0.98	1.36	1.24	1.19 ± 0.2
Contamination index				
Cd	>141	>168	>147	>152
PLI	>9.1	>11.1	>11.5	>10.6
ERI	>216	>263	>248	>242

This multi-elemental approach highlights significant soil contamination at the Monte Romero site, particularly with Ag, Sb, and Pb. The slag mass (~1080 tons) confined in the small smelting workshop area (~600 m^2) suggests a localized contamination footprint. However, erosion processes pose the potential threat of dispersing the contaminants over a broader area. This raises concerns about the potential spread of contamination beyond the immediate vicinity, affecting nearby soils and water sources. While the current ecological risk assessment categorizes the situation as moderate, the potential negative impact on the surrounding environment warrants further investigation.

5. Conclusions

Ancient metallurgical practices left a distinct geochemical signature on the local soil environment of Monte Romero. Trace element analysis unveiled significant concentrations of Ag, Cu, As, Pb, Sb, and Bi in soil samples adjacent to pre-Roman slag sites compared to a control area. This enrichment can be ascribed to post-depositional weathering processes involving the free-silica, ball-shaped slags scattered throughout the site, remnants of silver and copper smelting activities dating back to the Tartessian period (c. 7th century BC).

The presence of secondary Cu and Pb arsenates within the slag cavities suggests the breakdown of primary metallurgical phases, leading to the subsequent release and redistribution of potentially harmful elements. Consequently, the surrounding soil acts as a reservoir for these contaminants, exhibiting severe contamination primarily driven by Pb, Sb, and Ag, along with a moderate ecological risk associated with As, Pb, and Cu.

These findings underscore the long-lasting environmental repercussions of historical smelting operations on soil quality and the need to implement proper management strategies for archaeological sites hosting remnants of metal production.

Supplementary Materials: The following supporting information can be downloaded at: https://www.mdpi.com/article/10.3390/soilsystems8030078/s1, Table S1: Quality control report.

Author Contributions: Conceptualization, J.C.F.-C. and J.A.P.-M.; methodology, J.C.F.-C. software, J.C.F.-C.; validation, J.C.F.-C. and J.A.P.-M.; formal analysis, J.C.F.-C.; investigation, J.C.F.-C. and J.A.P.-M.; data curation, J.C.F.-C.; writing—original draft preparation, J.C.F.-C.; writing—review and editing, J.A.P.-M.; visualization, J.C.F.-C. All authors have read and agreed to the published version of the manuscript.

Funding: This research received no external funding.

Institutional Review Board Statement: Not applicable.

Informed Consent Statement: Not applicable.

Data Availability Statement: The authors confirm that the data supporting the findings of this study are available within the manuscript and its Supplementary Material (Table S1).

Conflicts of Interest: The authors declare no conflicts of interest.

References

1. Kibblewhite, M.; Toth, G.; Hermann, T. Predicting the preservation of cultural artefacts and buried materials in soil. *Sci. Total Environ.* **2015**, *529*, 249–263. [CrossRef] [PubMed]
2. Maskall, J.; Withehead, K.; Gee, C.; Thornton, I. Long-term migration of metals at historical smelting sites. *Appl. Geochem.* **1996**, *11*, 43–51. [CrossRef]
3. Amnai, A.; Radola, D.; Choulet, F.; Buatier, M.; Gimbert, F. Impact of ancient iron smelting wastes on current soils: Legacy contamination, environmental availability and fractionation of metals. *Sci. Total Environ.* **2021**, *776*, 145929. [CrossRef] [PubMed]
4. Asare, M.O.; Afriyie, J.O. Ancient mining and metallurgy as the origin of Cu, Ag, Pb, Hg, and Zn contamination in soils: A review. *Water Air Soil Pollut.* **2021**, *232*, 240. [CrossRef]
5. Gee, C.; Ramsey, M.H.; Maskall, J.; Thornton, I. Mineralogy and weathering processes in historical smelting slags and their effect on the mobilisation of lead. *J. Geochem. Explor.* **1997**, *58*, 249–257. [CrossRef]
6. Camizuli, E.; Scheifler, R.; Garnier, S.; Monna, F.; Losno, R.; Gourault, C.; Hamm, G.; Lachiche, C.; Delivet, G.; Chateau, C.; et al. Trace metals from historical mining sites and past metallurgical activity remain bioavailable to wildlife today. *Sci. Rep.* **2018**, *8*, 3436. [CrossRef] [PubMed]
7. Lottermoser, B.G. Mobilization of heavy metals from historical smelting slag dumps, north Queensland, Australia. *Min. Mag.* **2002**, *66*, 475–490. [CrossRef]
8. Kennedy, S.A.; Kelloway, S.J. Heavy metals in archaeological soils. The application of portable X-ray fluorescence (pXRF) spectroscopy for assessing risk to human health at industrial sites. *Adv. Archaeol. Pract.* **2021**, *9*, 145–159. [CrossRef]
9. Costagliola, P.; Benvenuti, M.; Chiarantini, L.; Bianchi, S.; Di Benedetto, F.; Paolieri, M.; Rossato, L. Impact of ancient metal smelting on arsenic pollution in the Pecora River Valley, Southern Tuscany, Italy. *Appl. Geochem.* **2008**, *23*, 1241–1259. [CrossRef]
10. Lottermoser, B.G. Evaporative mineral precipitates from a historical smelting slag dump, Río Tinto, Spain. *Neues Jb. Miner. Abh.* **2005**, *181*, 183–190. [CrossRef]
11. Chopin, E.I.B.; Alloway, B.J. Trace element partitioning and soil particle characterisation around mining and smelting areas at Tharsis, Ríotinto and Huelva, SW Spain. *Sci. Total Environ.* **2007**, *373*, 488–500. [CrossRef] [PubMed]
12. Fernández-Landero, S.; Fernández-Caliani, J.C.; Giráldez, I.; Morales, E.; Barba-Brioso, C.; González, I. Soil contaminated with hazardous waste materials at Rio Tinto mine (Spain) is a persistent secondary source of acid and heavy metals to the environment. *Minerals* **2023**, *13*, 456. [CrossRef]
13. Pérez Macías, J.A. *Metalurgia Extractiva Prerromana en Huelva*; Universidad de Huelva: Huelva, Spain, 1996; pp. 79–169.
14. Pérez Macías, J.A. *Las Minas de Huelva en la Antigüedad*; Diputación Provincial de Huelva: Huelva, Spain, 1998; pp. 48–96.
15. Strauss, G.K.; Madel, J.; Fernández Alonso, F. Exploration practice for strata-bound volcanogenic sulphide deposits in the Spanish-Portuguese Pyrite Belt: Geology, Geophysics, and Geochemistry. In *Time- and Strata-Bound Ore Deposits*; Klemm, D.D., Schneider, H.J., Eds.; Springer: Berlin, Germany, 1977; pp. 55–93.
16. Fernández Jurado, J.; Ruiz Mata, D. La metalurgia de la plata en época tartésica en Huelva. *Pyrenae* **1985**, *21*, 23–44.
17. Rothenberg, B.; García-Palomero, F. The Rio Tinto enigma—No more. Institute for Archaeo-Metallurgical Studies (IAMS). *Newsletter* **1986**, *8*, 3–5.
18. Matos, J.X.; Martins, A.; Rego, M.; Mateus, A.; Pinto, A.; Figueiras, J.; Silva, E. Roman slag distribution in the Portuguese sector of the Iberian Pyrite Belt. In Proceedings of the Actas V Congreso Internacional sobre Minería y Metalurgia Históricas en el Suroeste Europeo, León, Spain, 19–21 June 2008; pp. 567–576.
19. Álvarez-Valero, A.M.; Pérez-López, R.; Nieto, J.M. Prediction of the environmental impact of modern slags: A petrological and chemical comparative study with Roman age slags. *Am. Min.* **2009**, *94*, 1417–1427. [CrossRef]
20. Van Geen, A.; Adkins, J.F.; Boyle, E.A.; Nelson, C.H.; Palanqués, A. A 120-yr record of widespread contamination from mining of the Iberian Pyrite Belt. *Geology* **1997**, *25*, 291–294. [CrossRef]

21. Fernández-Caliani, J.C. La contaminación del suelo por la minería metálica de la Faja Pirítica Ibérica. *Macla* **2022**, *26*, 1–2.
22. Fernández-Caliani, J.C.; Barba-Brioso, C.; González, I.; Galán, E. Heavy metal pollution in soils around the abandoned mine sites of the Iberian Pyrite Belt (South-West Spain). *Water Air Soil Pollut.* **2009**, *200*, 211–226. [CrossRef]
23. Conde, C.; Tornos, F. Geochemistry and architecture of the host sequence of the massive sulfides in the northern Iberian Pyrite Belt. *Ore Geol. Rev.* **2020**, *127*, 103042. [CrossRef]
24. Pinedo Vara, I. *Piritas de Huelva. Su Historia, Minería y Aprovechamiento*; Summa: Madrid, Spain, 1963; pp. 403–409.
25. Junta de Andalucía. *Mapa de Suelos de Andalucía a Escala 1:400,000*; Instituto Andaluz de Reforma Agraria y Consejo Superior de Investigaciones Científicas: Madrid, Spain, 1989.
26. Rothenberg, B.; Blanco, A. *Studies in Ancient Mining and Metallurgy in South-West Spain: Explorations and Excavations in the Province of Huelva*; Institute for Archaeo-Metallurgical Studies (IAMS): London, UK, 1981.
27. Rothenberg, B.; Andrews, P.; Keesman, I. Monte Romero September 1986—The discovery of a unique Phoenician silver smelting workshop in south west-Spain. Institute for Archaeo-Metallurgical Studies (IAMS). *Newsletter* **1986**, *9*, 1–4.
28. Pérez Macías, J.A. Las minas de Tarteso, Tartesos. In *El Emporio del Metal*; Campos, J.M., Alvar, J., Eds.; Almuzara: Córdoba, Spain, 2013; pp. 449–472.
29. Junta de Andalucía. Resolución de 28 de julio de 2005, de la Dirección General de Bienes Culturales, por la que se resuelve inscribir colectivamente, con carácter genérico, en el Catálogo General del Patrimonio Histórico Andaluz, treinta y siete yacimientos arqueológicos y poblados amurallados de la Sierra de Aracena y Picos de Aroche, provincia de Huelva. *Bol. Off. Junta Andal.* **2005**, *166*, 46–57.
30. Kassianidou, V. The production of silver in Monte Romero, a 7th Century B.C. workshop in Huelva, Spain. *Pap. Inst. Archaeol.* **1993**, *4*, 37–47. [CrossRef]
31. Kassianidou, V. Early extraction of silver from complex polymetallic ores. In *Mining and Metal Production through the Ages*; Craddock, P., Lang, J., Eds.; The British Museum Press: London, UK, 2003; pp. 198–206.
32. Pérez Macías, J.A. La fundición protohistórica de Monte Romero en Almonaster la Real, Huelva. *Cuad. Suroeste* **1991**, *2*, 99–131.
33. *ISO/IEC 17025:2017*; General Requirements for the Competence of Testing and Calibration Laboratories. International Organization for Standardization (ISO): Geneva, Switzerland, 2017.
34. Häkanson, L. An ecological risk index for aquatic pollution control: A sedimentological approach. *Water Res.* **1980**, *14*, 975–1001. [CrossRef]
35. Tomlinson, D.L.; Wilson, J.G.; Harris, C.R.; Jeffrey, D.W. Problems in the assessment of heavy-metal levels in estuaries and the formation of a pollution index. *Helgol. Mar. Res.* **1980**, *33*, 566–575. [CrossRef]
36. Abrahim, G.M.S.; Parker, R.J. Assessment of heavy metal enrichment factors and the degree of contamination in marine sediments from Tamaki Estuary, Auckland, New Zealand. *Environ. Monit. Assess.* **2008**, *136*, 227–238. [CrossRef] [PubMed]
37. Salkield, L.V. Ancient slag in the south west of the Iberian Peninsula. In *La Minería Hispana e Iberoamericana. Contribución a su estudio*; Cátedra de San Isidoro: León, Spain, 1970; pp. 85–99.
38. Rovira, S.; Hunt, M.A. "Free silica" type slags of silver production in the Iberian Peninsula. In Proceedings of the 34th International Symposium on Archaeometry, Zaragoza, Spain, 3–7 May 2004; Diputación de Zaragoza: Zaragoza, Spain, 2006; pp. 217–222.
39. Álvarez-Valero, A.; Pérez-López, R.; Matos, J.; Capitán, M.A.; Nieto, J.M.; Sáez, R.; Delgado, J.; Caraballo, M. Potential environmental impact at São Domingos mining district (Iberian Pyrite Belt, SW Iberian Peninsula): Evidence from a chemical and mineralogical characterization. *Environ. Geol.* **2008**, *55*, 1797–1809. [CrossRef]
40. Ettler, V.; Johan, Z.; Kríbek, B.; Sebek, O.; Mihaljevic, M. Mineralogy and environmental stability of slags from the Tsumeb smelter, Namibia. *Appl. Geochem.* **2009**, *24*, 1–15. [CrossRef]
41. Nelson, H.; Shchukarev, A.; Sjöberg, S.; Lövgren, L. Composition and solubility of precipitated copper(II) arsenates. *Appl. Geochem.* **2011**, *26*, 696–704. [CrossRef]
42. Kabata-Pendias, A.; Mukherjee, A.B. *Trace Elements from Soils to Humans*; Springer: Berlin, Germany, 2007; p. 42.